

Elsevier Editorial(tm) for Engineering Applications of Artificial
Intelligence

Manuscript Draft

Manuscript Number:

Title: Neural Network Based Sliding Mode Control of Electronic Throttle

Article Type: Paper recommended from IFAC event

Keywords: electronic throttle control; uncertainty; sliding mode; neural
networks; adaptive control

Corresponding Author: Mr. Miroslav Baric Swiss Federal Institute of Technology

Other Authors: Ivan Petrovic, PhD; Nedjeljko Peric, PhD. University of Zagreb, Faculty of
Electrical Engineering and Computing, University of Zagreb, Faculty of Electrical
Engineering and Computing

Neural Network Based Sliding Mode Control of Electronic Throttle

Miroslav Barić^{a,*} Ivan Petrović^a Nedjeljko Perić^a

^a*Department of Control and Computer Engineering in Automation, Faculty of
Electrical Engineering and Computing, University of Zagreb, CROATIA*

Abstract

In this paper a neural network based sliding mode controller for electronic throttle is proposed. Electronic throttle is considered as an uncertain linear system. The uncertainties, which consist of an unknown friction and spring torque are estimated by the neural network whose parameters are adapted in an on-line fashion. Control and adaptive laws guarantee the boundedness of all signals in the system. Presented experimental results demonstrate the efficiency and robustness of the proposed control scheme.

Key words: electronic throttle control, uncertainty, sliding mode, neural networks, adaptive control

1 Introduction

Originally used only in high-performance vehicles with traction control, electronic throttle control (ETC) today becomes standard part of modern automotive systems. By replacing the mechanical link between the driver's pedal and the throttle valve, electronic throttle eliminates the need for the additional idle-speed actuator, since the idle-speed control can also be achieved through the ETC system. In general, ETC makes the engine control easier and thus introduces a possibility for the improvements in the sense of vehicle emission, fuel economy and drivability. These are the main reason for the significant interest of the control community for the ETC problem. A good survey of ETC can be found in [1].

* Corresponding author.

Email addresses: baric@control.ee.ethz.ch (Miroslav Barić),
ivan.petrovic@fer.hr (Ivan Petrović), nedjeljko.peric@fer.hr (Nedjeljko Perić).

The requirements set before ETC are high: the tracking of the referent valve opening should be as accurate as possible and at the same time the control system should be highly robust. Electronic throttles are produced in large series from cheap components, meaning that considerable variations in their electro-mechanical characteristics can be expected. Furthermore, significant variations of the throttle physical parameters may occur during its operation, mainly due to the changes of the temperature of the environment. Therefore, in order to meet the above mentioned requirements, it is natural to consider an ETC strategy based on robust and/or adaptive control concepts.

Sliding mode controllers have been used since 1950's in a variety of control applications [2–4]. The attractive feature of this control strategy is that a system in the sliding mode is insensitive to parameter variations and disturbances as long as these are implicit to the control input, i.e. as long as the matching condition is satisfied. This is particularly convenient for the ETC since the major uncertainty present in the electronic throttle (armature coil resistance) satisfies the "matching" condition [5]. Classical sliding mode control concept introduces discontinuous control action, which results in higher energy consumptions and may lead to the undesired oscillatory behavior known as "chattering" [3]. In order to achieve stable sliding mode behavior, at least the upper bound of the uncertainties and disturbances affecting the system must be known. This, however, may result with very conservative controller. In order to alleviate these disadvantages, the application of artificial neural networks in the sliding mode control has been considered [6–10].

In this paper an application of the neural network based sliding mode controller to the ETC is described. Neural network (NN) is used for the on-line estimation of the state-dependent uncertainties in the system, similar to the algorithm proposed in [6]. Adaptation algorithm is derived using the ideas introduced by Polycarpou *et. al.* in [11,12], guaranteeing the ultimate boundedness of the neural network parameters and all signals in the closed-loop system. The efficiency of the proposed algorithm has been experimentally verified.

The paper is structured as follows. In Section 2 the model of the electronic throttle is described. The proposed algorithm is given in Section 3. Experimental results are presented in Section 4. The concluding remarks are given in Section 5.

2 Electronic Throttle

Electronic throttle (ET) system is shown in Fig. 1. Main parts of the system are: DC motor, reduction gear box and a valve supported by a dual spring

system, consisting of two return springs, whose characteristic is depicted in Fig. 3. DC drive is supplied from the bipolar chopper. Motor shaft rotation is

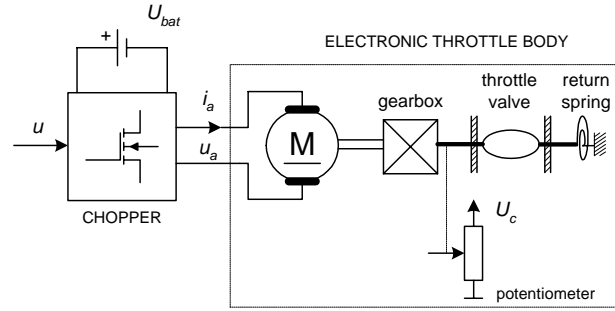


Fig. 1. Block scheme of the electronic throttle system

transmitted through the reduction gear box (see Fig. 2(b)) to the shaft with the throttle valve (Fig. 2(a)). The opening of the throttle valve determines the air mass inflow to the engine manifold. DC motor torque is in balance with the torque produced by the dual spring system. This is a standard fail-safe mechanism made for electronic subsystem failure situations, when the springs keep the throttle valve at the default position which ensures the air inflow just enough for the engine to keep running. This default position of the valve is called "Limp-Home position" (LH-position, θ_{LH} on Fig. 3).

Dynamic behavior of the electronic throttle is described by the following state space equations:

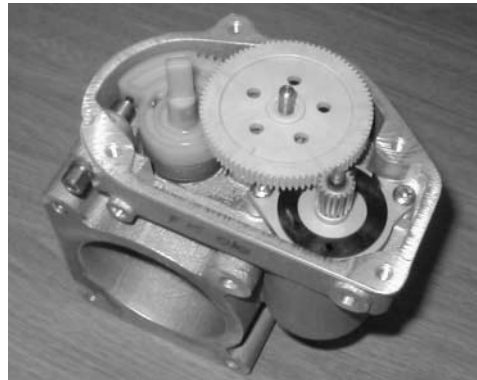
$$\dot{\theta} = \frac{1}{K_l} \omega_m, \quad (1)$$

$$\dot{\omega}_m = \frac{K_t}{J} i_a - \frac{K_l}{J} m_s(\theta) - \frac{1}{J} m_f(\omega_m), \quad (2)$$

$$\dot{i}_a = -\frac{K_a K_v}{T_a} \omega_m - \frac{1}{T_a} i_a + \frac{K_a}{T_a} u_a, \quad (3)$$



(a) Throttle valve



(b) Reduction gear box

Fig. 2. Electronic throttle

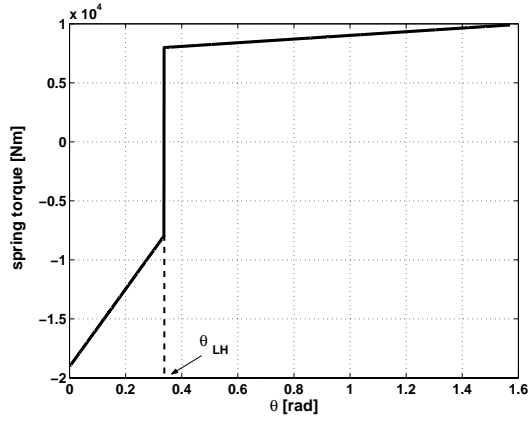


Fig. 3. Characteristic of the dual spring system

with the following notation: θ - valve angle, ω_m - DC motor angular velocity, i_a - DC motor armature current, u_a - DC motor armature voltage, m_s - spring torque, m_f - gear friction torque, K_a - armature gain, T_a - armature time constant, K_t - motor torque constant, K_v - electro-motive force constant, K_l - gear ratio.

Block diagram of the throttle model given by (1)-(3) is shown in Fig. 4. In this

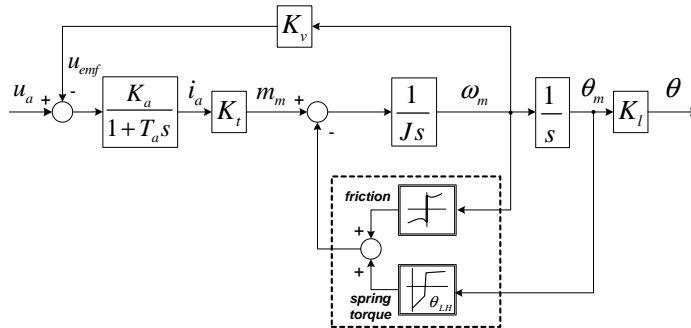


Fig. 4. Block diagram of the electronic throttle model

model it is assumed that the friction torque (m_f) depends only on the motor angular velocity ω_m , which is a satisfactory approximation. More accurate and detailed description of the friction model can be found in [1].

The dynamics of the armature current can be neglected, i.e. the equation (3) can be replaced by

$$i_a = K_a(u_a - K_v \omega_m). \quad (4)$$

The result is the reduced set of equations:

$$\dot{\theta} = \frac{1}{K_l} \omega_m, \quad (5)$$

$$\dot{\omega}_m = -\frac{K_t K_v K_a}{J} \omega_m + \frac{K_t K_a}{J} u_a - \frac{K_l}{J} m_s(\theta) - \frac{1}{J} m_f(\omega_m). \quad (6)$$

During the operation of the ET there are significant changes in the coefficient K_a due to the thermal variations of the armature resistance. This effect, together with the spring torque (m_s), the friction (m_f) and the disturbance caused by the air flow (m_L), represents the net uncertainties and disturbances (ξ) in the system:

$$\xi = \frac{1}{J} [-K_t K_v \Delta K_a \omega_m + K_t \Delta K_a u_a - K_l m_s(\theta) - m_f(\omega_m) - m_L]. \quad (7)$$

In order to solve the ETC problem, the value of ξ should be estimated. A control algorithm that uses a neural network for the estimation of ξ is presented in the following section.

3 Neural network based sliding mode controller

Consider a system described by the following equations:

$$\dot{\mathbf{x}} = \mathbf{A}\mathbf{x}(t) + \mathbf{B}\mathbf{u}(t) + \boldsymbol{\xi}(\mathbf{x}, \mathbf{u}, t), \quad (8)$$

where $\mathbf{A} \in \mathbb{R}^{n \times n}$, $\mathbf{B} \in \mathbb{R}^{n \times m}$, and $\boldsymbol{\xi}$ represents the uncertainty and unknown disturbances in the system.

Specifically, for the ET system described by (5) to (7) it can be written:

$$\mathbf{A} = \begin{bmatrix} 0 & 1/K_l \\ 0 & -K_t K_v K_a / J \end{bmatrix}, \quad \mathbf{B} = \begin{bmatrix} 0 & K_t K_a / J \end{bmatrix}^T,$$

$$\mathbf{x} = \begin{bmatrix} \theta & \omega_m \end{bmatrix}^T, \quad \mathbf{u} = [u_a], \quad \boldsymbol{\xi}(\mathbf{x}, \mathbf{u}, t) = \begin{bmatrix} 0 & \xi(\mathbf{x}, \mathbf{u}, t) \end{bmatrix}^T.$$

It is assumed that all states of the system are available and that function $\boldsymbol{\xi}(\mathbf{x}, \mathbf{u}, t)$ is bounded. The objective is to design a controller which will reduce the influence of joint uncertainties / disturbances $\boldsymbol{\xi}$ and achieve the tracking of the referent state vector \mathbf{x}_R . In this section, an adaptive sliding mode controller is considered. The design of the controller follows the usual procedure in the sliding mode control design: first, the control action is chosen, which will drive the system into the sliding mode and then, the parameters of the sliding surface are selected, such that the stable sliding behavior is ensured.

3.1 Driving the system into sliding mode

Consider the sliding surface \mathcal{S} defined as:

$$\mathcal{S} = \{\mathbf{x} : \mathbf{S}\mathbf{x}(t) - \boldsymbol{\phi}(t) = \mathbf{0}\}, \quad (9)$$

where $\mathbf{S} \in \mathbb{R}^{m \times n}$ is a design matrix and $\boldsymbol{\phi}(t)$ is a continuous function depending on the reference \mathbf{x}_R . The definition of the function $\boldsymbol{\phi}(t)$ is generally system- and goal-specific and will be given later for the ETC problem. In this phase of the controller design the goal is to confine the motion of the system states into the subspace defined by (9), or to bound it inside some neighborhood of the surface (9).

In order to stabilize the sliding motion on the surface \mathcal{S} , the following Lyapunov function candidate is considered:

$$V = \frac{1}{2} \mathbf{s}^T(t) \mathbf{s}(t), \quad (10)$$

where

$$\mathbf{s}(t) = \mathbf{S}\mathbf{x}(t) - \boldsymbol{\phi}(t). \quad (11)$$

Quadratic stability of the sliding mode will be achieved if the following holds:

$$\dot{V}(t) = -\mathbf{P}_s \mathbf{s}^T(t) \mathbf{s}(t), \quad (12)$$

where \mathbf{P}_s is a positive definite matrix. Time derivative of $V(t)$ is:

$$\dot{V}(t) = \mathbf{s}^T(t) [\mathbf{S}\mathbf{A}\mathbf{x}(t) + \mathbf{S}\mathbf{B}\mathbf{u}(t) + \mathbf{S}\boldsymbol{\xi} - \dot{\boldsymbol{\phi}}(t)]. \quad (13)$$

From (12) and (13) the following stabilizing control law is obtained:

$$\mathbf{u}_a(\mathbf{x}, t) = -(\mathbf{S}\mathbf{B})^{-1} [\mathbf{S}\mathbf{A}\mathbf{x}(t) + \mathbf{S}\boldsymbol{\xi} - \dot{\boldsymbol{\phi}}(t)] - (\mathbf{S}\mathbf{B})^{-1} \mathbf{P}_s \mathbf{s}(t). \quad (14)$$

Stabilizing control law as given by (14) cannot be realized since $\boldsymbol{\xi}$ is unknown. Instead, consider the following control law:

$$u_a(\mathbf{x}, t) = -(\mathbf{S}\mathbf{B})^{-1} [\mathbf{S}\mathbf{A}\mathbf{x}(t) + \mathbf{S}\hat{\boldsymbol{\phi}}_{NN}(\mathbf{x}, t) - \dot{\boldsymbol{\phi}}(t)] - (\mathbf{S}\mathbf{B})^{-1} \mathbf{P}_s \mathbf{s}(t). \quad (15)$$

In (15) the signal $\boldsymbol{\xi}(\mathbf{x})$ is replaced by the neural network $\hat{\boldsymbol{\phi}}_{NN}(\mathbf{x})$. Note that the neural network output is a function of only system states \mathbf{x} and that it cannot ideally replace the signal $\boldsymbol{\xi}(\mathbf{x}, \mathbf{u}, t)$, which depends both on states and control input and also includes external disturbances. Therefore, instead of the stability, control law (15) can guarantee only the boundedness of $\mathbf{s}(t)$.

In this paper a multilayer perceptron neural network (MLP NN) with a single hidden layer is used for $\hat{\boldsymbol{\phi}}_{NN}(\mathbf{x})$. It is known that for such a network a universal

approximation property holds [13]. MLP with one hidden layer is described by the following relations:

$$\mathbf{y}_0 = \mathbf{x}_{NN}, \quad (16)$$

$$\mathbf{x}_l = \begin{bmatrix} \mathbf{y}_{l-1} \\ 1 \end{bmatrix}, \quad \mathbf{v}_l = \mathbf{W}_l \mathbf{x}_l, \quad \mathbf{y}_l = \psi_l(\mathbf{v}_l), \quad l = 1, 2 \quad (17)$$

$$\hat{\phi}_{NN} = \mathbf{y}_2. \quad (18)$$

where $\mathbf{x}_{NN} \in \mathbb{R}^{n_0}$ denotes a network input vector, $\mathbf{x}_l \in \mathbb{R}^{n_{l-1}+1}$ is input to the l^{th} layer, \mathbf{y}_l is the l^{th} layer output and ψ_l represents the activation function of the l^{th} layer. n_l is a number of neurons in the l^{th} layer. The first layer is usually called *hidden layer* and the second one *the output layer*. In this paper full state vector will be used as an input vector, i. e. $\mathbf{x}_{NN} = \mathbf{x}$. As an activation function of the output layer linear function $\psi_2(\mathbf{v}_2) = \mathbf{v}_2$ is used. The activation function of the hidden layer $\psi_1(\mathbf{v}_1)$ will be defined later in the text.

It is necessary to define an adaptation law for the network parameters, $\dot{\hat{\mathbf{W}}}_1$ and $\dot{\hat{\mathbf{W}}}_2$, and the control law $\mathbf{u}(t)$, such that both the boundedness of $\mathbf{s}(t)$ and the boundedness of the neural network parameters $\hat{\mathbf{W}}_1$ and $\hat{\mathbf{W}}_2$ are ensured. The procedure that follows is based on the concepts developed by Lewis *et. al.* [14] and Polycarpou *et. al.* [12].

Based on the universal approximation property of the single hidden layer neural network, for a given network structure (i.e. the number of hidden neurons), there exists a set of optimal parameters \mathbf{W}_1 and \mathbf{W}_2 , for which the approximation error ϵ_{NN} is minimal on a compact region \mathcal{D} :

$$\phi_{NN}(\mathbf{W}_1, \mathbf{W}_2, \mathbf{x}) = \arg \min_{\hat{\mathbf{W}}_1, \hat{\mathbf{W}}_2} \left\{ \sup_{\mathbf{x} \in \mathcal{D}} \|\xi(\mathbf{x}, \mathbf{u}, t) - \phi_{NN}(\hat{\mathbf{W}}_1, \hat{\mathbf{W}}_2, \mathbf{x})\| \right\} \quad (19)$$

Uncertainties ξ can be approximated by this "ideal" network:

$$\xi(\mathbf{x}, \mathbf{u}, t) = \phi_{NN}(\mathbf{x}) + \epsilon_{NN}^*(\mathbf{x}, \mathbf{u}, t), \quad (20)$$

where ϵ_{NN}^* represents the approximation error of the "ideal" network $\phi_{NN}(\mathbf{x})$. Optimal parameters of the neural network are considered to be constant and unknown. Parameters of the "real" neural network $\hat{\phi}_{NN}$ used in the control law, namely $\hat{\mathbf{W}}_1$ and $\hat{\mathbf{W}}_2$, are approximations of unknown optimal parameters \mathbf{W}_1 and \mathbf{W}_2 . Expression (20) can be written as:

$$\xi(\mathbf{x}, \mathbf{u}, t) = \tilde{\phi}_{NN}(\mathbf{x}) + \hat{\phi}_{NN}(\mathbf{x}) + \epsilon_{NN}^*(\mathbf{x}, \mathbf{u}, t), \quad (21)$$

where $\tilde{\phi}_{NN}(\mathbf{x}, \mathbf{u}, t) = \phi_{NN}(\mathbf{x}) - \hat{\phi}_{NN}(\mathbf{x})$.

In order to define the neural network adaptation law, it is convenient to find the expression for $\tilde{\phi}_{NN}$ which is linear in parameters $\hat{\mathbf{W}}_1$ and $\hat{\mathbf{W}}_2$. Taylor

expansion of the hidden layer output may be written in the form:

$$\boldsymbol{\psi}_1(\mathbf{v}_1) = \boldsymbol{\psi}_1(\hat{\mathbf{v}}_1) + \boldsymbol{\Psi}'(\hat{\mathbf{v}}_1)(\mathbf{W}_1 - \hat{\mathbf{W}}_1)\mathbf{x}_1 + \mathbf{r}_2(\mathbf{W}_1), \quad (22)$$

where $\mathbf{r}_2(\mathbf{W}_1)$ represents higher order terms and $\boldsymbol{\Psi}'(\hat{\mathbf{v}}_1)$ is Jacobian:

$$\boldsymbol{\Psi}'(\hat{\mathbf{v}}_1) = \text{diag} \left\{ \frac{d\psi_i(\hat{v}_{1i})}{d\hat{v}_{1i}} \right\}, \quad (23)$$

where \hat{v}_{1i} denotes the i^{th} component of the vector $\hat{\mathbf{v}}_1$. The error $\tilde{\boldsymbol{\phi}}_{NN}$ can be written in the following manner:

$$\begin{aligned} \tilde{\boldsymbol{\phi}}_{NN} &= \mathbf{W}_2\boldsymbol{\psi}_1(\mathbf{v}_1) - \hat{\mathbf{W}}_2\boldsymbol{\psi}_1(\hat{\mathbf{v}}_1) = \\ &= \tilde{\mathbf{W}}_2 \left[\boldsymbol{\psi}_1(\hat{\mathbf{v}}_1) - \boldsymbol{\Psi}'(\hat{\mathbf{v}}_1)\hat{\mathbf{W}}_1\mathbf{x}_1 \right] + \\ &+ \hat{\mathbf{W}}_2\boldsymbol{\Psi}'(\hat{\mathbf{v}}_1)\tilde{\mathbf{W}}_1\mathbf{x}_1 + \boldsymbol{\Delta}(\hat{\mathbf{W}}_1, \hat{\mathbf{W}}_2, \mathbf{x}_1), \end{aligned} \quad (24)$$

where $\tilde{\mathbf{W}}_1 = \mathbf{W}_1 - \hat{\mathbf{W}}_1$, $\tilde{\mathbf{W}}_2 = \mathbf{W}_2 - \hat{\mathbf{W}}_2$ and:

$$\boldsymbol{\Delta}(\hat{\mathbf{W}}_1, \hat{\mathbf{W}}_2, \mathbf{x}_1) = \tilde{\mathbf{W}}_2\boldsymbol{\Psi}'(\hat{\mathbf{v}}_1)\mathbf{v}_1 + \mathbf{W}_2\mathbf{r}_2(\mathbf{W}_1). \quad (25)$$

Expression (24) is the desired form of $\tilde{\boldsymbol{\phi}}_{NN}$, linear in parameters $\hat{\mathbf{W}}_1$ and $\hat{\mathbf{W}}_2$. From (22) and (25) it follows:

$$\boldsymbol{\Delta}(\hat{\mathbf{W}}_1, \hat{\mathbf{W}}_2, \mathbf{x}_1) = \mathbf{W}_2[\boldsymbol{\psi}_1(\mathbf{v}_1) - \boldsymbol{\psi}_1(\hat{\mathbf{v}}_1)] - \hat{\mathbf{W}}_2\boldsymbol{\Psi}'(\hat{\mathbf{v}}_1)\mathbf{v}_1 + \mathbf{W}_2\boldsymbol{\Psi}'(\hat{\mathbf{v}}_1)\hat{\mathbf{v}}_1. \quad (26)$$

Finally, the following inequality holds:

$$\|\boldsymbol{\Delta}\|_2 \leq \rho_\Delta \sigma(\hat{\mathbf{W}}_1, \hat{\mathbf{W}}_2, \mathbf{x}_1), \quad (27)$$

where $\rho_\Delta = \max \{\|\mathbf{W}_1\|_F, \|\mathbf{W}_2\|_F\}$ and:

$$\begin{aligned} \sigma(\hat{\mathbf{W}}_1, \hat{\mathbf{W}}_2, \mathbf{x}_1) &= \max_{\mathbf{v}_1, \hat{\mathbf{v}}_1} \{ \|\boldsymbol{\psi}_1(\mathbf{v}_1) - \boldsymbol{\psi}_1(\hat{\mathbf{v}}_1)\|_2 \} + \|\boldsymbol{\Psi}'(\hat{\mathbf{v}}_1)\hat{\mathbf{v}}_1\|_2 + \\ &+ \|\hat{\mathbf{W}}_2\boldsymbol{\Psi}'(\hat{\mathbf{v}}_1)\|_F \|\mathbf{x}_1\|_2, \end{aligned} \quad (28)$$

where $\|\cdot\|_F$ denotes Frobenius norm. The term $\sigma(\hat{\mathbf{W}}_1, \hat{\mathbf{W}}_2, \mathbf{x}_1)$ is known, while ρ_Δ will be estimated in an on-line fashion by the parameter $\hat{\rho}_\Delta$. Parameter adaptation and control law are defined by the following Theorem:

Theorem 1 *Let the feedback control law for the system (8) be given by:*

$$\begin{aligned} \mathbf{u}(\mathbf{x}, t) &= -(\mathbf{S}\mathbf{B})^{-1} \left[\mathbf{S}\mathbf{A}\mathbf{x}(t) + \mathbf{S}\hat{\boldsymbol{\phi}}_{NN}(\mathbf{x}) - \dot{\boldsymbol{\phi}}(t) + \right. \\ &+ \hat{\rho}_\Delta \bar{\sigma}(\hat{\mathbf{W}}_1, \hat{\mathbf{W}}_2, \mathbf{x}_1) \mathbf{S} \tanh \left(\frac{\bar{\sigma}(\hat{\mathbf{W}}_1, \hat{\mathbf{W}}_2, \mathbf{x}_1) \mathbf{S}^T \mathbf{s}(t)}{\delta} \right) \left. \right] - \\ &- (\mathbf{S}\mathbf{B})^{-1} \mathbf{P}_s \mathbf{s}(t), \end{aligned} \quad (29)$$

with: \mathbf{P}_s positive definite, $\bar{\sigma}(\cdot) \triangleq 1 + \sigma(\cdot)$ and $\delta > 0$. \mathbf{x}_1 denotes the input to the hidden network layer.

Let the adaptation law of the parameters $\hat{\mathbf{W}}_1$, $\hat{\mathbf{W}}_2$ and $\hat{\rho}_\Delta$ be given by the following equations:

$$\dot{\hat{\mathbf{W}}}_1^T = \mathbf{P}_{W1}^{-1} \left[\mathbf{x}_1 \mathbf{s}(t) \mathbf{S} \hat{\mathbf{W}}_2 \Psi'(\hat{\mathbf{v}}_1) - \alpha_{W1} (\hat{\mathbf{W}}_1 - \hat{\mathbf{W}}_{10})^T \right], \quad (30)$$

$$\dot{\hat{\mathbf{W}}}_2^T = \mathbf{P}_{W2}^{-1} \left[(\psi_1(\hat{\mathbf{v}}_1) - \Psi'(\hat{\mathbf{v}}_1) \hat{\mathbf{v}}_1) \mathbf{s}(t) \mathbf{S} - \alpha_{W2} (\hat{\mathbf{W}}_2 - \hat{\mathbf{W}}_{20})^T \right], \quad (31)$$

$$\dot{\hat{\rho}}_\Delta = \frac{1}{\gamma_\rho} \left[\bar{\sigma}(\hat{\mathbf{W}}_1, \hat{\mathbf{W}}_2, \mathbf{x}_1) \mathbf{s}(t) \mathbf{S} \tanh \left(\frac{\bar{\sigma}(\hat{\mathbf{W}}_1, \hat{\mathbf{W}}_2, \mathbf{x}_1) \mathbf{S}^T \mathbf{s}(t)}{\delta} \right) - \alpha_\rho (\hat{\rho}_\Delta - \hat{\rho}_{\Delta 0}) \right], \quad (32)$$

where \mathbf{P}_{W1} and \mathbf{P}_{W2} are positive definite matrices, $\hat{\mathbf{W}}_{10}$, $\hat{\mathbf{W}}_{20}$ and $\hat{\rho}_{\Delta 0}$ are initial values of $\hat{\mathbf{W}}_1$, $\hat{\mathbf{W}}_2$ and $\hat{\rho}_\Delta$ respectively, and $\gamma_\Delta, \alpha_{W1}, \alpha_{W2}, \alpha_{\rho_\Delta} > 0$ are constant parameters.

With the control law (29) and the adaptive laws (30)-(32), with the stable dynamics defined for $\mathbf{s}(t) \equiv \mathbf{0}$, all the signals in the closed loop system are bounded.

PROOF. Proof is given in Appendix A.

Remark 1 Initial values for the network parameters could be determined by the preliminary training, or simply set to 0. If all network weights are set to 0, it is important to select an activation function of the hidden layer such that $\psi(0) \neq 0$. In this memo tanh with offset $\Delta\nu$ is used:

$$\psi(\nu) = \frac{1 - \exp(-2(\nu + \Delta\nu))}{1 + \exp(-2(\nu + \Delta\nu))}, \quad (33)$$

Remark 2 Initially, parameter $\hat{\rho}_\Delta$ should be set to 0. This parameter determines the level of "discontinuity" in the control action. If the uncertainty in the system is dominantly a function of system states, the growth of this parameter should be carefully controlled by the proper choice of γ_ρ and α_ρ , in order to benefit more from the neural network approximation and get smoother control action. If larger influence of the control vector dependent uncertainties and/or external disturbances is expected, more "discontinuous" control action should be allowed by selecting smaller parameter δ .

With the described neural network training and the control law given by (29), the system is driven close to the ideal sliding regime. The next step in the control design is to choose matrix \mathbf{S} and function $\phi(t)$ (see (9)) such that the stable reference tracking is achieved for the system in sliding mode.

3.2 Sliding mode dynamics

Assuming that the stability of the sliding mode is achieved, i.e. $\mathbf{s}(t) \mapsto \mathbf{0}$, matrix \mathbf{S} and function $\phi(\mathbf{x}_R)$ are defined in a way that will ensure asymptotic tracking of the reference vector \mathbf{x}_R .

System equations (5) and (6) are more conveniently written as:

$$\dot{\theta} = a_{12}\omega_m, \quad (34)$$

$$\dot{\omega}_m = a_{22}\omega_m + b_2u_a - \xi, \quad (35)$$

with:

$$a_{12} = \frac{1}{K_l}, \quad a_{22} = -\frac{K_t K_v K_a}{J}, \quad b_2 = \frac{K_t K_a}{J}. \quad (36)$$

Let the matrix \mathbf{S} be of the form:

$$\mathbf{S} = [s_1 \quad 1].$$

Then, sliding mode dynamics is governed by the following equation:

$$\dot{\theta} = -s_1 a_{12} \theta(t) + a_{12} \phi(t). \quad (37)$$

Tracking error $e(t)$ is given by:

$$e(t) = \theta(t) - \theta_R(t), \quad (38)$$

where $\theta_R(t)$ is the reference angle. From (37) and (38) follows the error dynamics in the sliding mode:

$$\dot{e}(t) = -s_1 a_{12} e(t) - s_1 a_{12} \theta_R(t) + a_{12} \phi(t) - \dot{\theta}_R(t). \quad (39)$$

By defining $\phi(\theta_R)$

$$\phi(\theta_R) = \frac{1}{a_{12}} (s_1 a_{12} \theta_R(t) + \dot{\theta}_R(t)) \quad (40)$$

equation (39) reduces to:

$$\dot{e}(t) = p_s e(t), \quad (41)$$

where $p_s = -s_1 a_{12}$ represents the pole of the sliding mode dynamics. The tracking dynamics is determined by the choice of s_1 . Obviously, in order to achieve stable tracking it is necessary that: $p_s < 0$.

4 Experimental results

The proposed ETC algorithm is implemented in a Matlab/Simulink environment as a C-mex file and experimental verification is carried out using Matlab's Real-Time Workshop running on Intel Celeron 700MHz PC. Sampling

time of the controller and the adaptation procedure is set to 0.5ms. Matlab's Runge-Kutta4 numerical integration procedure is used. In the experimental setup, throttle valve angle is measured using a low resolution potentiometer and 10-bit resolution A/D card. With such measurement setup it is possible to measure the throttle valve angle with the accuracy of 0.11° . Valve angular velocity is estimated using filtered differentiation. The following numerical values of the parameters are used: $P_{s1} = 500$, $\alpha_{W1} = \alpha_{W2} = 10^{-3}$, sliding mode pole $p_s = -40$, $P_{W1} = P_{W2} = 0.015$, $\gamma_\rho = 10^5$, $\delta = 2$. MLP neural network with 10 neurons in hidden layer is used. Inputs to the neural network are: measured valve angle θ and estimated valve velocity ω . All NN parameters and $\hat{\rho}_\Delta$ are initially set to 0.

Two sets of experiments have been performed. The goal of the first two experiments was to demonstrate the tracking performance of the proposed controller. Tracking of the sinusoidal and step referent signals of the small amplitude has been tested, in order to verify the ability of the controller to compensate the influence of the dual spring system and the friction. The second set of experiments was performed in order to check the robustness of the controller to drastic changes of the control gain (i.e. motor armature resistance).

Tracking performance of the controller is shown in Figs. 5-7. In all cases the

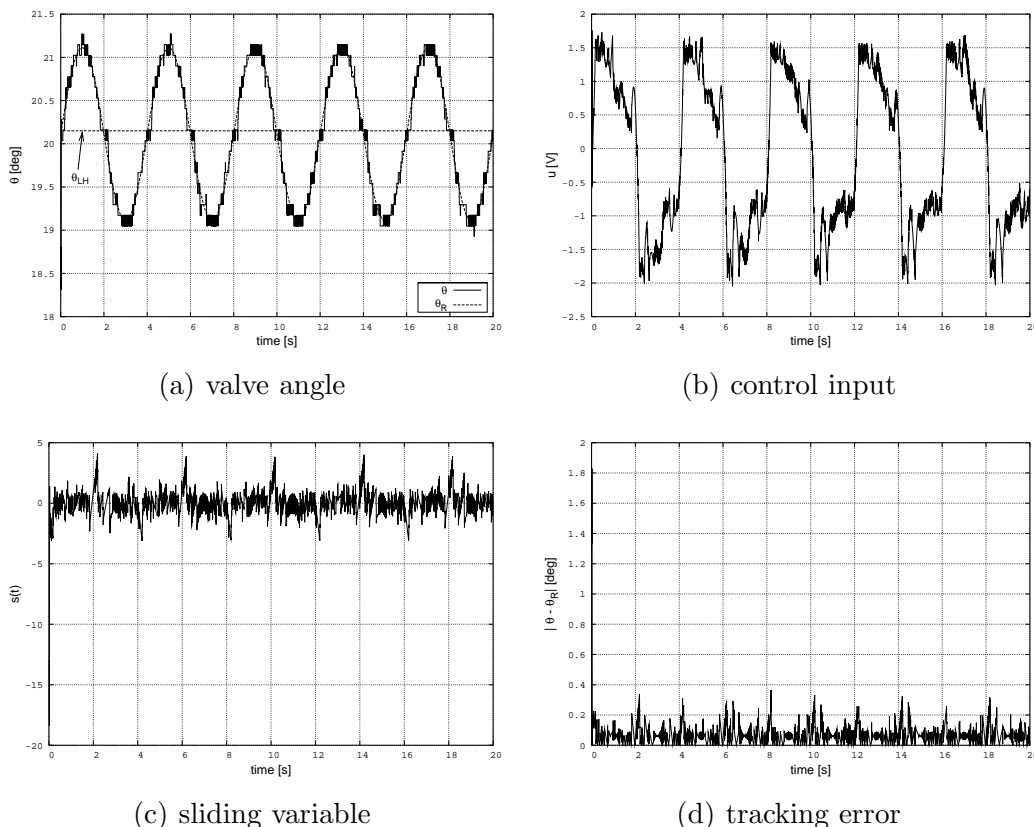


Fig. 5. Tracking sinus reference around LH.

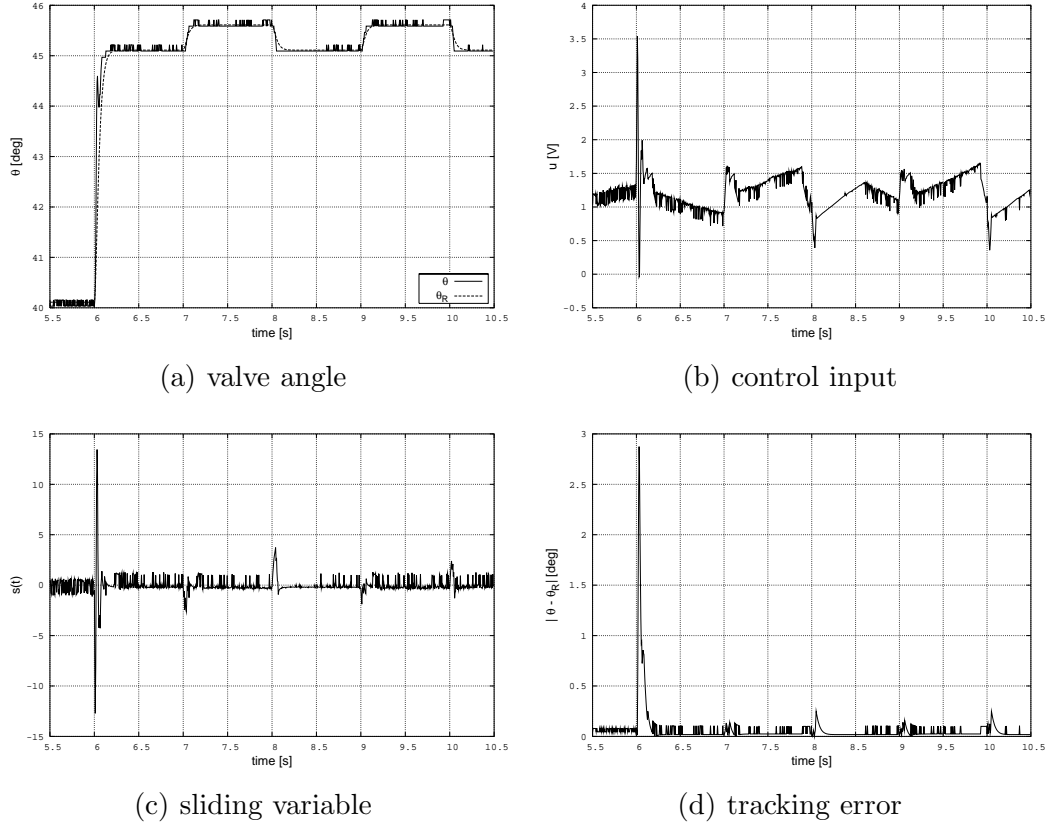


Fig. 6. Tracking step references above LH.

controller has successfully driven the tracking error below the resolution of the measurement. While tracking the sinusoidal reference around LH position, the controller successfully compensates the influence of the LH nonlinearity and the friction. The controller also shows very good performance in tracking small steps (see Figs. 6 and 7), demonstrating the ability to provide high tracking accuracy for small changes of the reference. This feature is very important in idle-speed control.

The change of the resistance is simulated in experiments by changing the control gain by factor of 2. Responses of the controller to both increase and decrease of the resistance are shown on Figs. 8-9. The results demonstrate that the controller is able to quickly adapt itself to extreme variations of the process dynamics.

5 Conclusion

In this paper a neural network based sliding mode controller for electronic throttle is considered. Uncertainties/disturbances consisting of unknown friction and spring torque are approximated with a neural network in an on-line

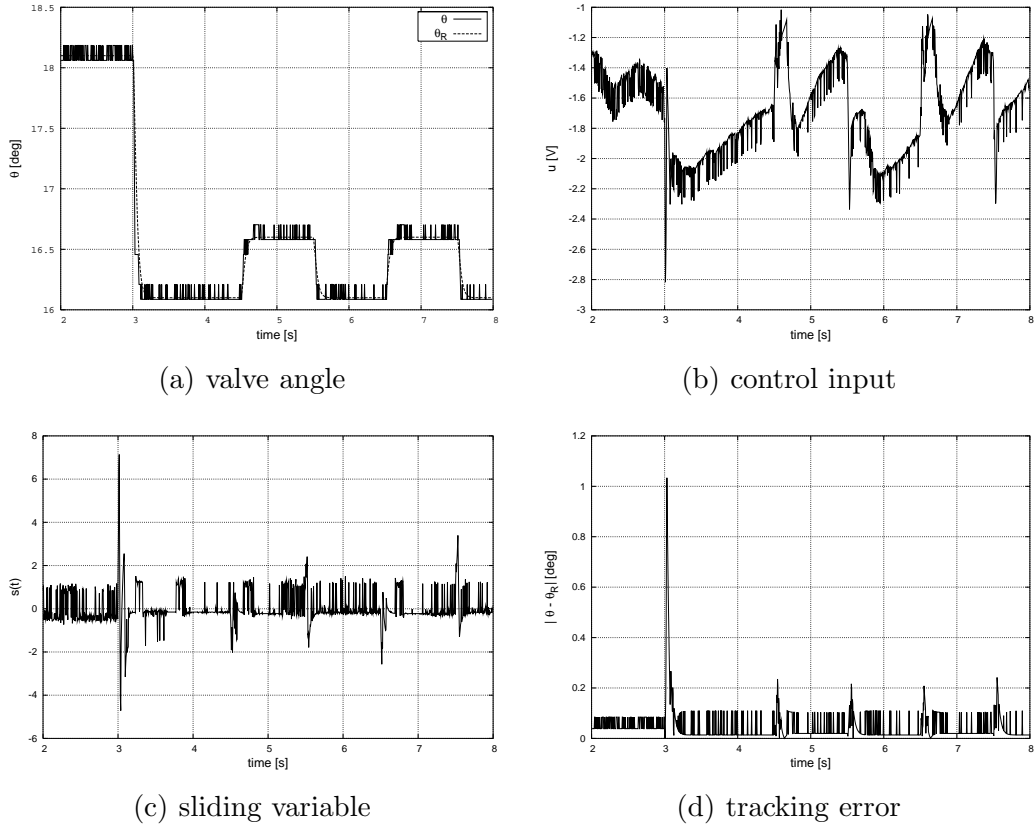


Fig. 7. Tracking step references below LH.

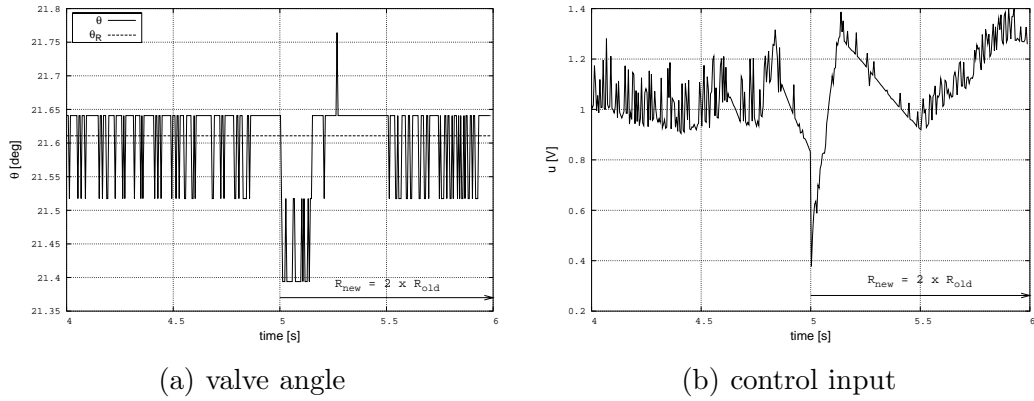


Fig. 8. Response with the increase of the armature resistance.

fashion. Control and adaptive laws guarantee the boundedness of all signals in the system. The proposed algorithm is successfully experimentally verified, showing a good performance. Control algorithm presented in this paper is generic in nature and can be successfully applied to other control problems in automotive industry. Its application is especially attractive in situations where large uncertainties and/or disturbances are expected. The authors will show through their future work other possible applications of the proposed control strategy.

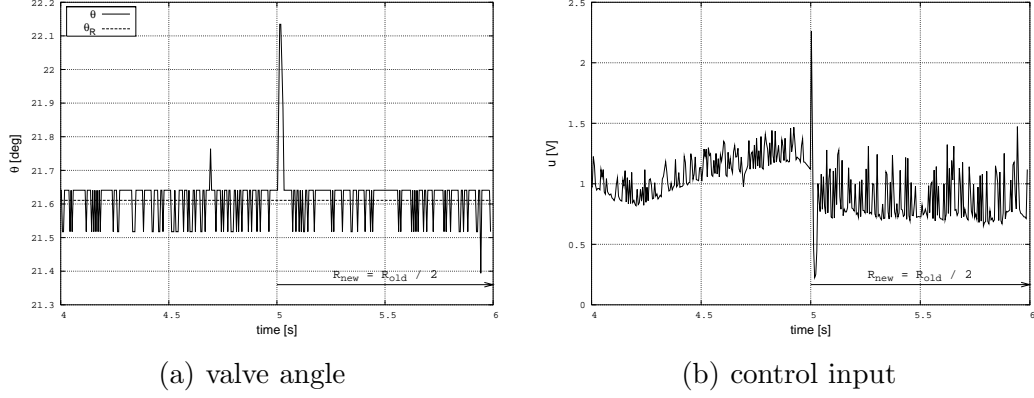


Fig. 9. Response with the decrease of the armature resistance.

Acknowledgements

Support from Ford Motor Company and the Ministry of Science and Technology of the Republic of Croatia is gratefully acknowledged.

A Proof of the Theorem 1

Consider the following Lyapunov function candidate:

$$V(t) = \frac{1}{2} \mathbf{s}^T(t) \mathbf{s}(t) + \frac{1}{2} \text{tr} \left\{ \tilde{\mathbf{W}}_1 \mathbf{P}_{W1} \tilde{\mathbf{W}}_1^T \right\} + \frac{1}{2} \text{tr} \left\{ \tilde{\mathbf{W}}_2 \mathbf{P}_{W2} \tilde{\mathbf{W}}_2^T \right\} + \frac{\gamma_\rho}{2} \tilde{\rho}_\Delta^2, \quad (\text{A.1})$$

where $\text{tr}\{\cdot\}$ is a matrix trace operator and $\tilde{\rho}_\Delta = \rho_\Delta - \hat{\rho}_\Delta$. Using the following relations:

$$\dot{\tilde{\mathbf{W}}}_1 = -\dot{\hat{\mathbf{W}}}_1, \quad \dot{\tilde{\mathbf{W}}}_2 = -\dot{\hat{\mathbf{W}}}_2, \quad \dot{\tilde{\rho}}_\Delta = -\dot{\hat{\rho}}_\Delta, \quad (\text{A.2})$$

$$\mathbf{y}^T \mathbf{x} = \text{tr} \left\{ \mathbf{x} \mathbf{y}^T \right\}, \quad \mathbf{x}, \mathbf{y} \in \mathbb{R}^n, \quad (\text{A.3})$$

and (29)-(32), it is easy to show that time derivative of (A.1) is given by:

$$\begin{aligned} \dot{V}(t) = & -\mathbf{s}^T(t) P_s \mathbf{s}(t) + \\ & + \alpha_{W1} \text{tr} \left\{ \tilde{\mathbf{W}}_1 \left(\hat{\mathbf{W}}_1 - \hat{\mathbf{W}}_{10} \right)^T \right\} + \\ & + \alpha_{W2} \text{tr} \left\{ \tilde{\mathbf{W}}_2 \left(\hat{\mathbf{W}}_2 - \hat{\mathbf{W}}_{20} \right)^T \right\} + \\ & + \alpha_\rho \tilde{\rho}_\Delta \left(\hat{\rho}_\Delta - \hat{\rho}_{\Delta 0} \right) + \mathbf{s}^T(t) \mathbf{S} \left[\mathbf{\Delta}(\mathbf{x}_1) + \boldsymbol{\epsilon}_{NN}^*(\mathbf{x}_1, \mathbf{u}, t) - \right. \\ & \left. - \bar{\sigma}(\hat{\mathbf{W}}_1, \hat{\mathbf{W}}_2, \mathbf{x}_1) \tanh \left(\frac{\bar{\sigma}(\hat{\mathbf{W}}_1, \hat{\mathbf{W}}_2, \mathbf{x}_1) \mathbf{S}^T \mathbf{s}(t)}{\delta} \right) \right]. \end{aligned} \quad (\text{A.4})$$

For the $tr\{\cdot\}$ in the (A.4) the following is valid:

$$\begin{aligned}
tr\left\{\tilde{\mathbf{W}}\left(\hat{\mathbf{W}}-\hat{\mathbf{W}}_0\right)^T\right\} &= tr\left\{\tilde{\mathbf{W}}\left(\mathbf{W}-\tilde{\mathbf{W}}-\hat{\mathbf{W}}_0\right)^T\right\}= \\
&= -\frac{1}{2}tr\left\{\tilde{\mathbf{W}}\tilde{\mathbf{W}}^T\right\}+tr\left\{\tilde{\mathbf{W}}\left(\mathbf{W}-\frac{1}{2}\tilde{\mathbf{W}}-\hat{\mathbf{W}}_0\right)^T\right\}= \\
&= -\frac{1}{2}tr\left\{\tilde{\mathbf{W}}\tilde{\mathbf{W}}^T\right\}+ \\
&\quad +tr\left\{\frac{1}{2}\left(\mathbf{W}-\hat{\mathbf{W}}_0+\hat{\mathbf{W}}_0-\hat{\mathbf{W}}\right)\left[\left(\mathbf{W}-\hat{\mathbf{W}}_0\right)-\left(\hat{\mathbf{W}}_0-\hat{\mathbf{W}}\right)\right]^T\right\}= \quad (\text{A.5}) \\
&= -\frac{1}{2}tr\left\{\tilde{\mathbf{W}}\tilde{\mathbf{W}}^T\right\}+\frac{1}{2}tr\left\{\left(\mathbf{W}-\hat{\mathbf{W}}_0\right)\left(\mathbf{W}-\hat{\mathbf{W}}_0\right)^T\right\}- \\
&\quad -\frac{1}{2}tr\left\{\left(\hat{\mathbf{W}}-\hat{\mathbf{W}}_0\right)\left(\hat{\mathbf{W}}-\hat{\mathbf{W}}_0\right)^T\right\}= \\
&= -\frac{1}{2}\|\tilde{\mathbf{W}}\|_F^2+\frac{1}{2}\|\mathbf{W}-\hat{\mathbf{W}}_0\|_F^2-\frac{1}{2}\|\hat{\mathbf{W}}-\hat{\mathbf{W}}_0\|_F^2,
\end{aligned}$$

Using (A.5) and (27) it can be shown that \dot{V} is bounded by:

$$\begin{aligned}
\dot{V}(t) &\leq -\mathbf{s}^T(t)\mathbf{P}_s\mathbf{s}(t)-\frac{\alpha_{W1}}{2}tr\left\{\tilde{\mathbf{W}}_1\tilde{\mathbf{W}}_1^T\right\}-\frac{\alpha_{W2}}{2}tr\left\{\tilde{\mathbf{W}}_2\tilde{\mathbf{W}}_2^T\right\}-\alpha_\rho\tilde{\rho}_\Delta^2+ \\
&\quad +\frac{\alpha_{W1}}{2}\left[\|\mathbf{W}_1-\hat{\mathbf{W}}_{10}\|_F-\|\hat{\mathbf{W}}_1-\hat{\mathbf{W}}_{10}\|_F\right]+ \\
&\quad +\frac{\alpha_{W2}}{2}\left[\|\mathbf{W}_2-\hat{\mathbf{W}}_{20}\|_F-\|\hat{\mathbf{W}}_2-\hat{\mathbf{W}}_{20}\|_F\right]+ \\
&\quad +\alpha_\rho\tilde{\rho}_\Delta\left(\rho_\Delta-\hat{\rho}_{\Delta 0}\right)+ \\
&\quad +\max\left\{\rho_\Delta,\epsilon_{NN}^*\left(\mathbf{x}\right)\right\}\left[\bar{\sigma}\left(\hat{\mathbf{W}}_1,\hat{\mathbf{W}}_2,\mathbf{x}_1\right)\|\mathbf{s}^T(t)\mathbf{S}\|_1-\right. \\
&\quad \left.-\bar{\sigma}\left(\hat{\mathbf{W}}_1,\hat{\mathbf{W}}_2,\mathbf{x}_1\right)\mathbf{s}^T(t)\mathbf{S}\tanh\left(\frac{\bar{\sigma}\left(\hat{\mathbf{W}}_1,\hat{\mathbf{W}}_2,\mathbf{x}_1\right)\mathbf{S}^T\mathbf{s}(t)}{\delta}\right)\right]. \quad (\text{A.6})
\end{aligned}$$

Using the following property [12]:

$$0 \leq |x| - x \tanh\left(\frac{x}{\delta}\right) \leq \kappa\delta, \quad (\text{A.7})$$

where $\kappa = 0.2785$, and well-known Rayleigh's inequality for symmetric positive definite matrices:

$$tr\left\{\mathbf{W}\mathbf{P}\mathbf{W}^T\right\} \leq \lambda_{max}(\mathbf{P})\|\mathbf{W}\|_F^2 = \lambda_{max}(\mathbf{P})tr\left\{\mathbf{W}\mathbf{W}^T\right\}, \quad (\text{A.8})$$

the following upper bound for \dot{V} is obtained:

$$\begin{aligned} \dot{V}(t) \leq & -\lambda_{\min}(\mathbf{P}_s) \mathbf{s}^T(t) \mathbf{s}(t) - \frac{\alpha_{W1}}{2\lambda_{\max}(\mathbf{P}_{W1})} \text{tr} \left\{ \tilde{\mathbf{W}}_1 \mathbf{P}_{W1} \tilde{\mathbf{W}}_1^T \right\} - \\ & - \frac{\alpha_{W2}}{2\lambda_{\max}(\mathbf{P}_{W2})} \text{tr} \left\{ \tilde{\mathbf{W}}_2 \mathbf{P}_{W2} \tilde{\mathbf{W}}_2^T \right\} - \alpha_\rho \hat{\rho}_\Delta^2 + \\ & + \frac{\alpha_{W1}}{2} \left\| \mathbf{W}_1 - \hat{\mathbf{W}}_{10} \right\|_F + \frac{\alpha_{W2}}{2} \left\| \mathbf{W}_2 - \hat{\mathbf{W}}_{20} \right\|_F + \\ & + \alpha_\rho \rho_\Delta (\rho_\Delta - \hat{\rho}_{\Delta 0}) + m\kappa\delta \max \{ \rho_\Delta, \|\boldsymbol{\epsilon}_{NN}^*\| \}, \end{aligned} \quad (\text{A.9})$$

where m is the dimension of the control vector \mathbf{u} . Finally, \dot{V} is bounded by:

$$\dot{V}(t) \leq -pV(t) + q, \quad (\text{A.10})$$

with

$$p = \min \left\{ 2\lambda_{\min}(\mathbf{P}_s), \frac{\alpha_{W1}}{\lambda_{\max}(\mathbf{P}_{W1})}, \frac{\alpha_{W2}}{\lambda_{\max}(\mathbf{P}_{W2})}, \frac{2\alpha_\rho}{\gamma_\rho} \right\} \quad (\text{A.11})$$

$$\begin{aligned} q = & \frac{\alpha_{W1}}{2} \left\| \mathbf{W}_1 - \hat{\mathbf{W}}_{10} \right\|_F + \frac{\alpha_{W2}}{2} \left\| \mathbf{W}_2 - \hat{\mathbf{W}}_{20} \right\|_F + \\ & + \alpha_\rho \rho_\Delta (\rho_\Delta - \hat{\rho}_{\Delta 0}) + m\kappa\delta \max \{ \rho_\Delta, \|\boldsymbol{\epsilon}_{NN}^*\| \} \end{aligned} \quad (\text{A.12})$$

From (A.10) it follows:

$$V(t) \leq \frac{q}{p} + \left[V(0) - \frac{q}{p} \right] \exp(-pt), \quad (\text{A.13})$$

Therefore, all signals in the system are bounded. \square

References

- [1] J. Deur, D. Pavković, N. Perić, M. Jansz, D. Hrovat, An electronic throttle control strategy including compensation of friction and limp-home effects, *IEEE Transactions on Industry Applications* 40 (3) (2004) 821–834.
- [2] V. I. Utkin, *Sliding Modes in Control and Optimization*, Springer, 1992.
- [3] V. I. Utkin, J. Guldner, J. Shi, *Sliding Mode Control in Electromechanical Systems*, Taylor and Francis, 1999.
- [4] C. Edwards, S. K. Spurgeon, *Sliding Mode Control: Theory and Applications*, Vol. Vol. 7 of Systems and Control Book Series, Taylor and Francis Ltd, 1998.
- [5] M. Yokoyama, K. Shimizu, N. Okamoto, Application of sliding-mode servo controllers to electronic throttle control, in: *Proceedings of the 37th IEEE Conference on Decision and Control (CDC98)*, Vol. 2, 1998, pp. 1541–1545.

- [6] H. Morioka, K. Wada, A. Šabanović, K. Jezernik, Neural-network based chattering free sliding mode control, in: Proc. of SICE annual conference, 1995, pp. 1303–1308.
- [7] G. Liu, V. Kadiramanathan, S. Billings, Neural network based variable structure control for nonlinear discrete systems, reserach report no. 626, Tech. rep., Dept. of Automatic Control & Systems Eng., The University of Sheffield (May 1996).
- [8] M. Ertugrul, O. Kaynak, Neuro sliding mode control of robotic manipulators, *Mechatronics* 10 (1-2) (2000) 243–267.
- [9] F.-Y. Lin, R.-J. Wai, Sliding-mode-controlled slider-crank mechanism with fuzzy neural network, *IEEE Trans. on Industrial Electronics* 48 (1) (2001) 60–70.
- [10] M. Barić, I. Petrović, N. Perić, Neural network based sliding mode controller for a class of linear systems with unmatched uncertainties, in: Proc. of the 41st IEEE Conference on Decision and Control (CDC02), 2002, pp. 967–972.
- [11] M. M. Polycarpou, P. Ioannou, Modeling, identification and stable adaptive control of continuous-time nonlinear dynamical systems using neural networks, in: Proc. of the 1992 American Control Conference, 1992, pp. 36–40.
- [12] M. M. Polycarpou, M. J. Mears, Stable adaptive tracking of uncertain systems using nonlinearly parametrized on-line approximators, *Int. J. Control* 70 (3) (1998) 363–384.
- [13] K. Funahashi, On the approximate realization of continuous mappings by neural networks, *Neural Networks* 2 (1989) 183–192.
- [14] F. Lewis, S. Jagannathan, A. Yeşildirek, *Neural Network Control of Robot Manipulators and Nonlinear Systems*, Taylor & Francis, 1999.